ChemComm

Genetic Encoding of A Nonhydrolyzable Phosphotyrosine Analog in Mammalian Cells

Journal:	*ChemComm*
Manuscript ID	CC-COM-03-2022-001578.R1
Article Type:	Communication

SCHOLARONE™
Manuscripts

Please do not adjust margins

COMMUNICATION

Genetic Encoding of A Nonhydrolyzable Phosphotyrosine Analog in Mammalian Cells

Received 00th January 20xx,
Accepted 00th January 20xx

DOI: 10.1039/x0xx00000x

Xinyuan He,[1,†] Bin Ma,[2] Yan Chen,[2] Jiantao Guo[2,3]* and Wei Niu[1,3]*

Protein tyrosine phosphorylation plays a critical role in signal transduction. We report the genetic incorporation of a phosphotyrosine (pTyr) analog, *p*-carboxymethyl-L-phenylalanine (CMF), into proteins in mammalian cells. This nonhydrolyzable pTyr analog can facilitate biological studies by removing complications caused by the dynamic interconversion between the phosphorylated and non-phosphorylated isoforms of a protein.

Protein tyrosine phosphorylation plays a pivotal role in many aspects of cell biology and is reversibly regulated by protein tyrosine kinases (PTKs) and protein tyrosine phosphatases (PTPs). In order to study protein tyrosine phosphorylation-associated cellular events, homogeneous proteins with site-specific phosphorylations are needed. While PTKs can be used to phosphorylate proteins *in vitro*, they have limited site specificity and often results in sub-stoichiometric phosphorylation.[1] In addition, it is challenging to identify suitable kinases for the *in vitro* modification of a large number of newly identified and putative phosphorylation sites. Semisynthetic (e.g., native chemical ligation) and cell-free methods have been developed to site-selectively introduce phosphotyrosine (pTyr).[2-6] In addition, genetic incorporation of phosphotyrosine (pTyr) or its precursor analog in live *E. coli* cells was recently reported.[7-9] Furthermore, synthesis of proteins containing nonhydrolyzable pTyr analogs, including *p*-carboxymethyl-L-phenylalanine (CMF) and 4-phosphomethyl-L-phenylalanine (Pmp), were also reported in *E. coli*.[7, 10] Nonhydrolyzable pTyr analogs that retain biological function but are resistant to hydrolysis by protein tyrosine phosphatases (PTPs) will greatly facilitate functional studies of tyrosine phosphorylation and associated cellular events. Indeed, the dynamic inter-conversion of phosphorylated and dephosphorylated isoforms can complicate interpretations of experimental data and further hinder deciphering the roles of individual phosphorylation sites.

A major barrier to the broad application of nonhydrolyzable pTyr analogs in biological studies is the lack of a method for their genetic encoding in live mammalian cells. Indeed, a method that enables efficient expression of proteins with defined and nonhydrolyzable tyrosine phosphorylation patterns in real-time is critical to investigations of cellular mechanisms in many pTyr-dependent signaling pathways. Here we report the first genetic incorporation of CMF, a nonhydrolyzable pTyr analog,[11-16] into proteins in mammalian cells. Functional replacement of pTyr by CMF was demonstrated using the human signal transducer and activator of transcription-1 (STAT1) as the model system. The method developed in this work will enhance one's ability to study pTyr-dependent events.

To genetically encode CMF in mammalian cells, an *E. coli* tyrosyl-tRNA synthetase (EcTyrRS) mutant library was constructed by randomizing four amino acid residues (Y37, L71, W129, and D182; Fig. S1a), based on the analysis of its crystal structure (PDB: 1X8X)[17]. These residues likely interact with the carboxylic acid side chain of CMF. The DNA library fragments were inserted after an ADH1 promoter in a yeast protein expression vector, which also encoded an amber suppressor tRNA derived from *E. coli* tyrosyl-tRNA (EctRNA$_{CUA}$). A library of 1×10^7 clones was obtained and its quality was verified by DNA sequencing (Fig. S1b).

The selection was conducted in *Saccharomyces cerevisiae* by following a previously established procedure (Fig. S1c).[18-19] Four clones (Fig. 1a) were obtained from the selection, from which two unique protein sequences were obtained as CMFRS-1 (Y37H, L71V, and D182G) and CMFRS-2 (Y37H, L71V, W129F, and D182G). Positions Tyr37, Leu71, and Asp182 showed a complete convergence to His, Val, and Gly, respectively, while position Trp129 either maintained the wild-type or changed to Phe. The evolved CMFRS shares two common mutations,

[a.] *Chemical and Biomolecular Engineering, University of Nebraska-Lincoln, Lincoln, Nebraska, 68588, United States. E-mail: wniu2@unl.edu*
[b.] *Department of Chemistry, University of Nebraska-Lincoln, Lincoln, Nebraska, 68588, United States. E-mail: jguo4@unl.edu*
[c.] *The Nebraska Center for Integrated Biomolecular Communication (NCIBC), University of Nebraska-Lincoln, Lincoln, Nebraska, 68588, United States.*
Electronic Supplementary Information (ESI) available: [details of any supplementary information available should be included here]. See DOI: 10.1039/x0xx00000x

Please do not adjust margins

Leu71Val and Asp182Gly, with a sTyrRS that we reported previously for the encoding of sulfotyrosine (sTyr) in mammalian cells.[20] Both mutations expand the active site in order to accommodate the large substituent at the *para*-position of Tyr. In addition, the D182G mutation eliminates the electrostatic repulsion between the negatively charged Asp and the substituent on Tyr.[20] The evolved CMFRSs was evaluated by analyzing the expression of green fluorescent proteins as the reporter in *S. cerevisiae* using a yeast GFP (yeGFP) with an amber mutation at position Asn149. As shown in Fig. 1b, significantly higher (p-value < 0.02) GFP fluorescence was observed in the presence of CMF for both variants. The more prevalent variant, CMFRS-1, led to higher reading. Our in vitro assay[20] (Fig. S2c) showed that the activity of CMFRS-1 was comparable to but lower than our previously evolved sTyrRS. Protein engineering with a more stable synthetase scaffold[21] may further improve its activity. CMFRS-1 was designated as CMFRS and chosen for all subsequent experiments.

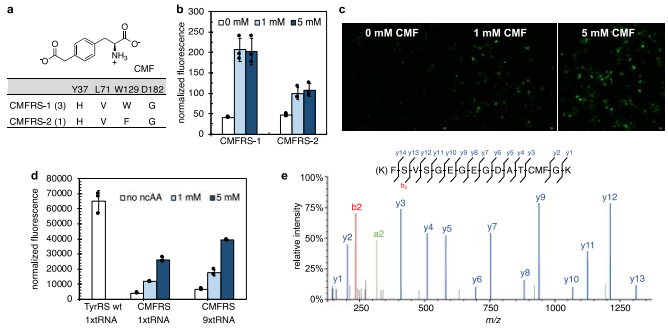

Fig. 1 Characterization of the evolved CMFRSs. **a.** Mutations in the evolved CMFRS variants. Numbers in parentheses represent the occurrence of the variant in library selection. The CMF is synthesized as a D, L mixture. **b.** Fluorescence readings of yeast cells expressing the evolved CMFRSs and an yeGFP mutant that contained an amber mutation at position N149. CMF was included in culture media at 0 mM (open bar), 1 mM (light blue bar), or 5 mM (dark blue bar). Fluorescence intensity was normalized to cell growth. **c.** Confocal images of 293T cells expressing the evolved CMFRS and an EGFP mutant that contained an amber mutation at position Tyr40. Scale bars, 10 mm. **d.** Flow cytometry analyses of 293T cells expressing the CMFRS or the wild-type EcTyrRS together with the EGFP-Y40TAG mutant. The normalized fluorescence was calculated by multiplying the mean fluorescence intensity by the percentage of fluorescent cells in flow cytometry analyses in the absence (open bar), 1 mM (light blue bar), or 5 mM (dark blue bar) of CMF. **e.** LC-MS/MS analysis of the tryptic peptide that contains the position of incorporation. **b** and **d** Data are plotted as the mean ± s.d. from n= 3 independent experiments.

The fidelity and the efficiency of CMFRS was further characterized in 293T cells. For protein expression experiments, the gene that encodes CMFRS was inserted behind a non-regulated CMV promoter on plasmid pCMFRS that contains an amber suppressor tRNA under the control of a human U6 promoter. The selective incorporation of CMF into proteins in 293T cells was then tested by suppression of an amber mutation in a C-terminal His6-tagged EGFP mutant, EGFP-Tyr40TAG, which was encoded on plasmid pEGFP. When cells reached 70% confluency, they were transiently transfected with pCMFRS and pEGFP. After 6 h of incubation at 37 ºC in a humidified atmosphere of 5% CO_2, fresh media was exchanged to include 1 mM or 5 mM CMF and the cells were grown for an additional 24 h. Fluorescence microscopy of the cells revealed that significant EGFP was only expressed in the presence of CMF. Little background expression was observed in the absence of CMF (Fig. 1c). Expression levels of EGFP were further quantified using flow cytometry analysis. As shown in Fig. 1d, the relative decoding efficiency of CMFRS in the presence of 5 mM CMF is about 40% of the efficiency of the wild-type EcTyrRS.

Incorporation of CMF into EGFP was further confirmed by mass spectrometry analysis of the full-length protein. To this end, the EGFP-Tyr40TAG mutant was expressed in 293T cells in the presence of 5 mM CMF, purified by affinity chromatography, and further separated from impurities by SDS-PAGE (Fig. S3a). A single major signal of 29705.7 Da was identified, which corresponds to EGFP protein with CMF following the loss of N-terminal Met and subsequent acetylation at the Val residue (expected mass 29705.9 Da, Fig. S3b). To further confirm the site-specific incorporation of CMF, peptide sequencing using tandem mass spectrometry (MS/MS) was performed (Fig. 1e). Following trypsin digest of purified EGFP, the peptide fragment that contained the position of incorporation was analyzed. Fragmentation data provided clear evidence that CMF was incorporated at position 40 of EGFP (Fig. 1e). Finally, the fidelity of incorporation by the evolved CMFRS was quantified based on the relative abundance of the modified and unmodified peptides (Fig. S3c). The precursor ions for peptide containing CMF (773.3395 m/z, [M+2H$^+$]) and peptide containing Tyr (752.3345 m/z, ([M+2H$^+$]) were extracted at 5 ppm mass accuracy.

Furthermore, we sought to optimize the decoding system. It was reported that the expression level of the tRNA is the limiting factor of decoding efficiency in mammalian cells.[22-23] To further increase the CMF incorporation, a series of pCMFRS plasmid variants with different copies of tRNA were constructed. These plasmids were co-transfected with plasmid pEGFP 2TAG that contains the EGFP-40TAG-150TAG for the evaluation of multi-site CMF incorporation in 293T cells. Fluorescence of EGFP was observed in the presence of both 1 mM and 5 mM CMF. Significantly higher (p < 0.01) level of expression was observed at 5 mM (Fig. S3d). Furthermore, the EGFP expression increases with increasing copies of tRNA (Fig. S3d). The CMFRS/9xtRNA plasmid was also examined together with plasmid pEGFP by flow cytometry. A decoding efficiency of around 60% of that of the wild-type EcTyrRS was observed (Fig. 1d). This construct was used in subsequent studies.

Next, we examined if functional replacement of pTyr with CMF can be realized in the human signal transducer and activator of transcription-1 (STAT1) protein. Phosphorylation at the Tyr701 position of STAT1 leads to its formation of a homodimer and binding to specific DNA sequences (e.g., IFN-γ-activated sequence) following nuclear translocation.[24] In this experiment, the DNA binding capability of the C-terminal fragment of STAT1 mutant containing CMF at position 701 (132-712, c-STAT1-701CMF) was studied *in vitro*. The c-STAT1-701CMF was expressed and purified from 293T cells (Fig. S4a). The site-specific incorporation of CMF at position 701 was verified by MS/MS analysis (Fig. S4b). The interaction between c-STAT1-701CMF mutant and a short M67 DNA fragment (Fig.

This journal is © The Royal Society of Chemistry 20xx

2) was examined by fluorescence-based electrophoretic mobility shift assay (EMSA). As shown in Fig. 2, gel shifting of DNA caused by protein binding was observed when c-STAT1-701CMF concentration reached 120 nM. Meanwhile, the control experiment using the unphosphorylated c-terminal fragment of the wild-type STAT1 protein (c-STAT1-701Tyr) did not lead to gel shifting in the presence of the same concentration of M67 DNA fragment. As a positive control, we generated c-STAT1-701pTyr (Fig. S6) from c-STAT1 by following a reported protocol[25] and conducted a side-by-side comparison between c-STAT1-701pTyr and c-STAT1-701CMF. As shown in Fig. S7, c-STAT1-701pTyr displayed slightly better binding affinity towards its DNA substrate than that of c-STAT1-701CMF. It should be noted that the purity of c-STAT1-701pTyr is around 80% (Fig. S6), which affects the apparent binding affinity. Nevertheless, the data suggest that c-STAT1-701CMF functioned similar to c-STAT1-701pTyr under the experimental conditions. We further tested the binding between additional two STAT1 variants, which has Asp (701D) or Glu (701E) mutation at position 701. Neither of the variants showed gel shifting effect at protein concentrations up to 240 nM (Fig. 2b). The findings confirmed that CMF is a better pTyr analog than negatively charged natural amino acids, i.e., Asp and Glu.

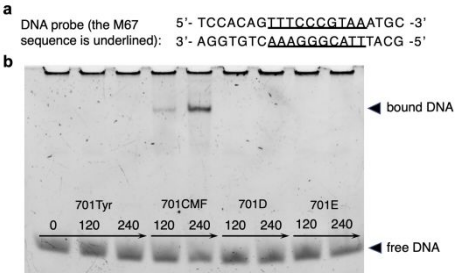

Fig. 2 Interaction between STAT1 and its DNA substrate. a. Sequence of the 21-bp DNA oligonucleotide duplex used in this study. The M67 site, which is recognized by STAT1 dimer following phosphorylation at Try701, is underlined. **b.** Fluorescence-based EMSA assay. The DNA concentration was fixed at 30 nM. The protein concentrations varied from 0 to 240 nM. Free and bound (DNA-protein complex) DNAs were visualized by SYBR® Gold EMSA nucleic acid gel stain. The original EMSA image is provided in Fig. S8.

To further demonstrate that the STAT1-701CMF mutant functions in a similar manner to naturally phosphorylated STAT1, we examined the behavior of STAT1-701CMF with phospho-STAT1 (pTyr701) antibody. We first conducted western blot experiments using the total lysate of 293T cells that expressed variants of the STAT1-EGFP fusion protein. As shown in Fig. 3a (lane 6), a protein band was clearly detected by the phospho-STAT1 (pTyr701) antibody when STAT1-EGFP-701TAG was expressed in the presence of CMF. The detected protein has a similar size to the phosphorylated STAT1-EGFP fusion protein, which was observed in interferon-γ (IFN-γ)-induced, STAT1-EGFP-expressing cells (lane 4, Fig. 3a). On the other hand, signal from cells expressing STAT1-EGFP-701TAG in the absence of CMF (lane 7, Fig. 3a) is close to background signal detected in the negative control, in which cells expressing STAT1-EGFP without the induction of IFN-γ (lane 5, Fig. 3a). Similar results were observed when residue at position 701 was mutated into Asp (701D, lane 2, Fig. 3a) or Glu (701E, lane 3, Fig. 3a). Further western blot experiments with anti-STAT1 antibody (independent of phosphorylation state) verified the expression and the correct size of STAT1-EGFP variants (lanes 8 to 14, Fig. 3a). A low level of expression was detected in the lysate of STAT1-EGFP-701TAG cells without exogenously added CMF (lane 14, Fig. 3a). The data confirmed that STAT1-701CMF can be recognized by phospho-STAT1 (pTyr701) antibody.

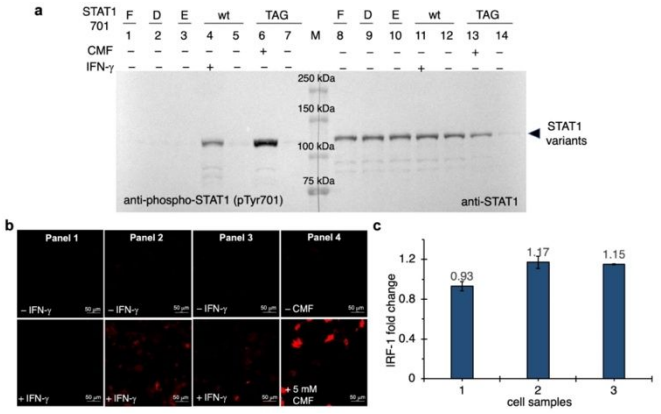

Fig. 3 Detection of STAT1 by phospho-STAT1 (pTyr701) antibody. (a) Western blot of cell lysates expressing STAT1 variants. Lanes 1 and 8, STAT1-EGFP-701F; lanes 2 and 9, STAT1-EGFP-701D; lanes 3 and 10, STAT1-EGFP-701E; lanes 4 and 11, wild-type STAT1-EGFP with IFN-γ induction; lanes 5 and 12, wild-type STAT1-EGFP without IFN-γ induction; lanes 6 and 13, STAT1-EGFP-701TAG with CMF; lanes 7 and 14, STAT1-EGFP-701TAG without CMF. Lane M is the molecular weight marker. The calculated molecular weight of STAT1-EGFP variants was 115.9 kDa. Lanes 1-7 were detected by phospho-STAT1 (pTyr701) antibody. Lanes 8-14 were detected by anti-STAT1 antibody. The original Western blot image is provided in Fig. S9. (b) Images of cells expressing STAT1 variants. Panel 1, 293T-ΔSTAT1 cells; Panel 2, 293T-ΔSTAT1 cells expressing wild-type STAT1; Panel 3, 293T-ΔSTAT1 cells expressing STAT1-701TAG and the wild-type EcTyrRS; Panel 4, 293T-ΔSTAT1 cells expressing STAT1-701TAG and the CMFRS. Immunofluorescence images were obtained by the treatment of permeabilized cells with phospho-STAT1 (pTyr701) antibody followed by anti-rabbit secondary antibody-Alex594 conjugate. Scale bars, 50 mm. The full set of images are provided in Fig. S10. (c) Gene expression analysis in 293T-ΔSTAT1 cells. The expression of IRF1 is regulated by the phosphorylation of STAT-1. Sample 1, cells expressing pSTAT1-701TAG and pTyrRS-wt, without IFN-γ; Sample 2, cells expressing pSTAT1-701TAG and pTyrRS-wt, with IFN-γ; Sample 3, cells expressing pSTAT1-701TAG and pCMFRS, with 5 mM CMF, without IFN-γ.

Next, we conducted cell-based immunofluorescence assay. In order to remove background signals from endogenously expressed STAT1, we first generated a STAT1 knockout cell line, 293T-ΔSTAT1, using CRISPR/Cas method (see details in Methods). Cells were treated and cultivated under indicated conditions (Fig. 3b), then fixed and permeabilized. The phospho-STAT1 (pTyr701) antibody was added as the primary antibody, followed by an Alexa Fluor 594-labeled secondary antibody. Cells were then visualized under the confocal microscope. As shown in the Panel 1 of Fig. 3b, no signal was detected with 293T-ΔSTAT1 cells either in the absence or in the presence of IFN-γ induction. This result confirmed the successful deletion of the STAT1-encoding gene in this cell line. Following transfection with pSTAT1, fluorescence was detected only in cells that were induced with IFN-γ (Panel 2, Fig. 3b), which verified a functional signaling pathway in the cell line. Meanwhile, strong signal was observed when STAT1-701TAG was expressed together with CMFRS in the presence of CMF (bottom Panel 4, Fig. 3b) and no fluorescent cells were detected

in the absence of CMF (top Panel 4, Fig. 3b). This observation is in line with control cells that expressed STAT1-701TAG together with the wild-type EcTyrRS, for which fluorescence was only detected in IFN-γ-induced cells (Panel 3, Fig. 3b). About three-fold stronger signal was detected in Panel 4 than those of Panel 2 and Panel 3, which indicates a larger amount of STAT1-701CMF than STAT1-701pTyr at the time of measurement. This is mainly due to the fact that STAT1-701pTyr is constantly dephosphorylated in live cells. In contrast, no hydrolysis can happen to STAT1-701CMF. Nevertheless, results of the immunofluorescence assay confirmed that CMF is chemically and/or structurally similar to pTyr.

Finally, we conducted gene expression studies to further examine the function of STAT1-701CMF. It is known that the expression of interferon regulatory factor-1 (IRF-1) can be stimulated by the activation of STAT1. Here we monitored IRF-1 expression level in the presence of two STAT1 variants. We first expressed wild-type STAT1 in 293T-ΔSTAT1 cells and used it in the control experiments. As shown in Fig. 3c, a 1.17-fold increase in IRF-1 expression was observed when the phosphorylation of wild-type STAT1 was induced by IFN-γ. In contrast, no elevated IRF-1 expression level was detected in the absence of IFN-γ. When STAT1-701TAG was expressed in the presence of CMF, a 1.15-fold increase in IRF-1 expression was observed without IFN-γ induction, which is comparable to that of wild-type STAT1 with IFN-γ induction. Since the accumulative amount of STAT1-701pTyr cannot be accurately measured due to constant dephosphorylation events, only qualitative comparison on transcription level changes of IRF-1 is possible. Nevertheless, the above experiments provide evidence that CMF can be used as an analog of pTyr in cellular studies albeit with a likely weaker ability to activate STAT1 than that of pTyr.

Overall, this work represents the first genetic encoding of a nonhydrolyzable pTyr analog in yeast and mammalian cells. In a proof-of-concept study using STAT1 as the model protein, we provided evidence to show that CMF could serve as a functional analog of pTyr in proteins expressed in mammalian cells. We expect our work not only to facilitate fundamental investigations, but also to accelerate biomedical applications that target protein tyrosine phosphorylation.

Author Contributions

X. He, B. Ma and Y. Chen contributed to investigation, methodology, analysis, and writing; W. Niu and J. Guo in conceptualization, project administration, supervision, and writing.

Conflicts of interest

There are no conflicts to declare.

Notes and references

1. P. V. Hornbeck, J. M. Kornhauser, S. Tkachev, B. Zhang, E. Skrzypek, B. Murray, V. Latham and M. Sullivan, *Nucleic Acids Res.*, 2012, **40**, D261-D270.
2. Z. Chen and P. A. Cole, *Curr. Opin. Chem. Biol.*, 2015, **28**, 115-122.
3. J. J. Ottesen, M. Huse, M. D. Sekedat and T. W. Muir, *Biochemistry*, 2004, **43**, 5698-5706.
4. J. P. Oza, M. B. Amrofell, M. C. Jewett, J. P. Oza, M. C. Jewett, J. P. Oza, M. C. Jewett, J. P. Oza, M. C. Jewett, H. R. Aerni, N. L. Pirman, K. W. Barber, S. Rogulina, J. Rinehart, H. R. Aerni, N. L. Pirman, K. W. Barber, S. Rogulina, F. J. Isaacs, J. Rinehart, H. C. M. ter, F. J. Isaacs and M. C. Jewett, *Nat. Commun.*, 2015, **6**, 8168.
5. M. Jbara, S. K. Maity, M. Morgan, C. Wolberger and A. Brik, *Angew. Chem., Int. Ed.*, 2016, **55**, 4972-4976.
6. S. Chen, R. Maini, X. Bai, R. C. Nangreave, L. M. Dedkova and S. M. Hecht, *J. Am. Chem. Soc.*, 2017, **139**, 14098-14108.
7. X. Luo, G. Fu, R. E. Wang, X. Zhu, C. Zambaldo, R. Liu, T. Liu, X. Lyu, J. Du, W. Xuan, A. Yao, S. A. Reed, M. Kang, Y. Zhang, H. Guo, C. Huang, P.-Y. Yang, I. A. Wilson, P. G. Schultz and F. Wang, *Nat. Chem. Biol.*, 2017, **13**, 845-849.
8. C. Fan, K. Ip and D. Soell, *FEBS Lett.*, 2016, **590**, 3040-3047.
9. C. Hoppmann, A. Wong, B. Yang, S. Li, T. Hunter, K. M. Shokat and L. Wang, *Nat. Chem. Biol.*, 2017, **13**, 842-844.
10. J. Xie, L. Supekova and P. G. Schultz, *ACS Chem. Biol.*, 2007, **2**, 474-478.
11. A. Guerra-Castellano, A. Diaz-Quintana, G. Perez-Mejias, C. A. Elena-Real, K. Gonzalez-Arzola, S. M. Garcia-Maurino, M. A. De la Rosa and I. Diaz-Moreno, *Proc. Natl. Acad. Sci. U. S. A.*, 2018, **115**, 7955-7960.
12. S. Subramanyam, M. Ismail, I. Bhattacharya and M. Spies, *Proc. Natl. Acad. Sci. U. S. A.*, 2016, **113**, E6045-E6054.
13. H. L. Rust, V. Subramanian, G. M. West, D. D. Young, P. G. Schultz and P. R. Thompson, *ACS Chem. Biol.*, 2014, **9**, 649-655.
14. N. A. Kalogriopoulos, I. Lopez-Sanchez, C. Lin, T. Ngo, K. K. Midde, S. Roy, N. Aznar, F. Murray, M. Garcia-Marcos, I. Kufareva, M. Ghassemian and P. Ghosh, *Proc. Natl. Acad. Sci. U. S. A.*, 2020, **117**, 28763-28774.
15. T. R. Burke, Jr., J. Luo, Z.-J. Yao, Y. Gao, H. Zhao, G. W. A. Milne, R. Guo, J. H. Voigt, C. R. King and D. Yang, *Bioorg. Med. Chem. Lett.*, 1999, **9**, 347-352.
16. L. Tong, T. C. Warren, S. Lukas, J. Schembri-King, R. Betageri, J. R. Proudfoot and S. Jakes, *J. Biol. Chem.*, 1998, **273**, 20238-20242.
17. T. Kobayashi, T. Takimura, R. Sekine, V. P. Kelly, K. Kamata, K. Sakamoto, S. Nishimura and S. Yokoyama, *J. Mol. Biol.*, 2005, **354**, 739.
18. J. W. Chin, T. A. Cropp, S. Chu, E. Meggers and P. G. Schultz, *Chem. Biol.*, 2003, **10**, 511-519.
19. H. S. Lee, J. Guo, E. A. Lemke, R. D. Dimla and P. G. Schultz, *J. Am. Chem. Soc.*, 2009, **131**, 12921-12923.
20. X. He, Y. Chen, D. G. Beltran, M. Kelly, B. Ma, J. Lawrie, F. Wang, E. Dodds, L. Zhang, J. Guo and W. Niu, *Nature Communications*, 2020, **11**, 4820.
21. K. T. Grasso, M. J. R. Yeo, C. M. Hillenbrand, E. D. Ficaretta, J. S. Italia, R. L. Huang and A. Chatterjee, *Biochemistry*, 2021, **60**, 489-493.
22. W. Wang, J. K. Takimoto, G. V. Louie, T. J. Baiga, J. P. Noel, K.-F. Lee, P. A. Slesinger and L. Wang, *Nat. Neurosci.*, 2007, **10**, 1063-1072.
23. W. H. Schmied, S. J. Elsasser, C. Uttamapinant and J. W. Chin, *J. Am. Chem. Soc.*, 2014, **136**, 15577-15583.
24. N. C. Reich, *JAKSTAT*, 2013, **2**, e27080.
25. U. Vinkemeier, S. L. Cohen, I. Moarefi, B. T. Chait, J. Kuriyan and J. E. Darnell, Jr., *EMBO J.*, 1996, **15**, 5616-5626.

This journal is © The Royal Society of Chemistry 20xx